



# A new ionic liquid organic redox electrolyte for high-efficiency iodine-free dye-sensitized solar cells

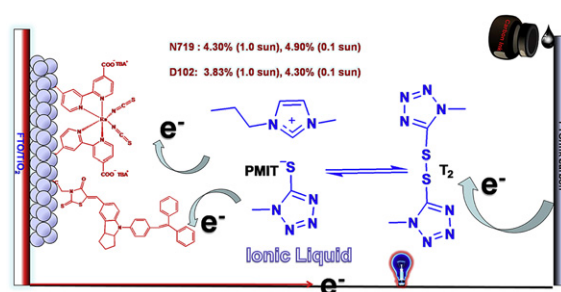
Hongwei Wu, Zhibin Lv, Shaocong Hou, Xin Cai, Dan Wang, Hany Kafafy, Yongping Fu, Chao Zhang, Zengze Chu, Dechun Zou\*

Beijing National Laboratory for Molecular Sciences, Key Laboratory of Polymer Chemistry and Physics of Ministry of Education, College of Chemistry and Molecular Engineering, Peking University, Beijing 100871, China

## HIGHLIGHTS

- A new iodine-free IL organic electrolyte is presented for using in DSSC.
- Ink carbon as the CE showed better catalytic activity than Pt.
- The organic dye D102 presented high energy conversion efficiency of 3.83%.

## GRAPHICAL ABSTRACT



## ARTICLE INFO

### Article history:

Received 1 April 2012

Received in revised form

19 June 2012

Accepted 19 July 2012

Available online 23 August 2012

### Keywords:

Ionic liquid

Dye-sensitized solar cells

Organic redox

Iodine-free

Ink carbon

## ABSTRACT

A new ionic liquid (IL) 5-mercapto-1-methyltetrazole 1-methyl-3-propylimidazolium salt PMIT with di-5-(1-methyltetrazole) disulfide ( $T_2$ ) as the organic redox couple is adopted for application in IL dye-sensitized solar cells (DSSCs). Adopting ultralow-cost and superior catalytic ink carbon as the counter electrode (CE), the N719- and D102-sensitized devices show high efficiencies of 4.30% and 3.83% under  $100 \text{ mW cm}^{-2}$  light illumination, respectively. Electrochemical studies provide insights on the mass-transfer and recombination kinetics of the electrolyte and electrochemical catalysis of the CE. The ink carbon CE exhibits more excellent catalytic activity than the Pt CE for the redox couple. These show an attractive prospect of carbon materials for application in DSSCs based on new iodine-free ionic liquid organic electrolyte.

© 2012 Elsevier B.V. All rights reserved.

## 1. Introduction

Renewable and green energy are important technological drivers of future economic development. Solar cell technology (photovoltaics) is one of the key technologies with the potential to meet the demand for green energy for sustainable development. Dye-

sensitized solar cells (DSSCs) [1] have higher efficiency and lower cost compared with numerous other solar cells. Extensive and effective systematic studies on DSSCs have been conducted worldwide since O'Regan and Grätzel reported significant breakthroughs in 1991 [1]. To further improve the photon-to-electricity conversion efficiency (PCE) of DSSCs, scientists and technicians have, in the past 20 years, made unremitting efforts in the optimization of DSSC component elements, including the optimization of the photoanode [2,3], the design and synthesis of broad-spectrum dye molecules with high absorption coefficients [4,5], and the development and

\* Corresponding author. Fax: +86 10 62759799.

E-mail address: [dczou@pku.edu.cn](mailto:dczou@pku.edu.cn) (D. Zou).

substitution of counter electrode (CE) materials with high catalytic activity by regulating the electrolyte composition [6,7]. To date, the DSSCs' PCE is as high as 12% [8]. This improvement shows that, as an effective photo-to-electricity conversion device, DSSCs have a huge potential in resolving the energy and environmental crises faced by humans. Traditional DSSCs based on triiodide/iodide ( $I_3^-/I^-$ ) redox couple are highly efficient [9,10]. However, they have some serious disadvantages, including CE corrosion (especially when silver grids are used as resistance in collecting current to reduce large devices), iodine sublimation, and visible light absorption. These disadvantages seriously restrict the mass production and commercial application of DSSCs [11,12]. To resolve the aforementioned problems, developing redox couples that are iodine-free, non-corrosive, and can weakly absorb visible light is very important in the future development of DSSCs. Currently, many iodine-free redox couple systems have been developed, consisting mainly of metal complexes (copper, nickel, and cobalt) [13–17], inorganic materials [ $Br^-/Br_3^-$  and  $SCN^-/(SCN)_3^-$ ] [18–20], and organic redox couples (TEMPO, thiolate/disulfide) [21–24]. Grätzel and co-workers [22] reported on an organic redox couple derived from 5-mercapto-1-methyltetrazole that gave a PCE of 6.4% in Z907-based liquid-state DSSCs under a standard illumination condition ( $100\text{ mW cm}^{-2}$ ). Wang and co-workers [25] adopted the redox couple of tris(1,10-phenanthroline) cobalt(II/III) to prepare liquid-state DSSCs based on the organic dye C218, and obtained a record energy conversion efficiency of 8.3% under standard illumination condition. In addition to the redox couple, the CE is another major component of DSSCs. Its catalytic activity has a significant impact on cell performance. Among numerous CE materials, platinum (Pt) is widely applied because of its superior electrocatalytic activity, high conductivity, and chemical stability. However, it also has some disadvantages, such as high cost, limited reserve, and corrosion from  $I_3^-/I^-$  electrolyte, which affect the cost-effective fabrication and long term stability of the devices. Therefore, the development of new CE materials is an important direction in the development of DSSCs. Recently, numerous CE materials have been developed in succession, including carbon materials (carbon spheres, activated carbon, porous carbon, and carbon nanotubes) [26–29], surface-nitrided nickel [30], CoS [31] and many others. DSSCs using all kinds of carbon materials as CE achieve very high PCEs. Murakami et al. [26] adopted carbon black as the CE, and the efficiency of DSSCs with an  $I_3^-/I^-$ -based liquid-state electrolyte reached 9.1%. Carbon materials have great potential in DSSC application because of their rich sources and cheap price. Another major challenge faced by DSSCs is the long-term stability of the devices. As previously mentioned, the traditional highly efficient liquid-state electrolyte of DSSCs normally uses acetonitrile as the solvent. This electrolyte is highly volatile, causing difficult encapsulation. The room temperature ionic liquid (RTIL) has been widely adopted in DSSCs and other electrochemical devices because of its good chemical and thermal stability, negligible vapor pressure, wide electrochemical window, and high ionic conductivity [20,32–34]. At present, DSSCs based on pure ionic liquid (IL) have reached PCEs of up to 8.2% [35]. However, it still adopts traditional  $I_3^-/I^-$  electrolyte and Pt CE and cannot address the problems inherent in these materials. Based on these considerations, the ideal choice for preparing efficient DSSCs is to adopt an iodine-free, purely IL redox couple with weak visible light absorption as the electrolyte and low-cost carbon materials as the CE. Currently, studies on this field are rare. Sun and co-workers recently reported on purely IL DSSCs by adopting the organic dye TH305 as sensitizer and a disulfide/thiolate as redox couple [36]. Unfortunately, the efficiency of the cells was only around 1% under standard illumination. Hence, we made efforts to continue this field. In the current study, we synthesized a new IL electrolyte composed of 5-mercapto-1-methyltetrazole-1-methyl-3-propylimidazolium salt

(PMIT)/di-5-(1-methyltetrazole) disulfide ( $T_2$ ) (Scheme 1). Based on this electrolyte, we prepared efficient iodine-free ion-liquid DSSCs using carbon materials as the CE. The efficiency of the N719-sensitized and organic dye D102-sensitized DSSCs under standard illumination condition ( $100\text{ mW cm}^{-2}$ ) is high 4.30% and 3.83%, respectively. To the best of our knowledge, the conversion efficiency is currently the highest for this type of DSSC. These new components may overcome the shortcomings of traditional liquid cells while effectively reducing the cost of DSSCs by adopting the low-price and highly catalytic ink carbon as the counter electrode. In addition, these new DSSCs show great potential in flexible and tandem solar cells under back illumination condition.

## 2. Experiment

### 2.1. Preparation of the DSSC $TiO_2$ photoanode

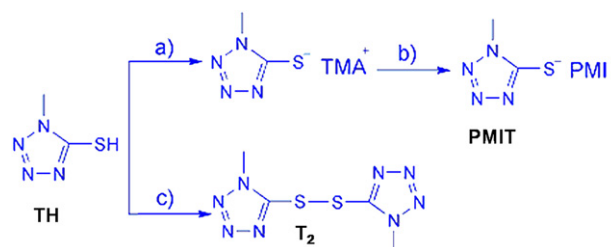
$TiO_2$  photoanodes 6  $\mu\text{m}$  thick (DHS-TPP200,  $\sim 20\text{ nm}$  diameter; Qiseguang Inc., Dalian, China) on fluorine-doped tin oxide (FTO) glass were prepared via screen printing. These photoanodes were sintered at  $150^\circ\text{C}$  for 15 min and at  $450^\circ\text{C}$  for 30 min. When the temperature of the final photoanode was reduced to  $100^\circ\text{C}$ , the photoanodes were immersed in an N719 (Solaronix) or D102 ethanol solution (0.5 mM) at room temperature for 24 h. The DSSCs were prepared by assembling the dye-sensitized photoanode and the CE into a sealed sandwich-type cell, which were separated using a 40  $\mu\text{m}$  thick hot-melt ionomer film (Surlyn, Dupont) as a spacer. The surface area of all devices was  $0.252\text{ cm}^2$ .

### 2.2. CE preparation

FTO glass plates with holes were subsequently cleaned with a detergent solution, water, and ethanol in an ultrasonic bath. The screen printing procedure was performed using a Pt paste (Hep-tachroma, DHS-PtSP) on the FTO glass plates. The printed CEs were heated in an oven at  $400^\circ\text{C}$  for 30 min. The dispersive ink carbon was purchased from Shanghai Ink Factory (Advanced Carbonic Ink, 234). The carbon electrodes were prepared by spin coating for 1 min at  $1000\text{ r min}^{-1}$  and heating in an oven at  $300^\circ\text{C}$  for 30 min. The grain size of the carbon particle is  $\sim 20\text{ nm}$ . The thickness of the carbon CE was approximately 700 nm (measured by the step profiler). The specific surface was  $30\text{ m}^2\text{ g}^{-1}$  (BET, ASAP 2010, Micrometer).

### 2.3. PMIT synthesis

The procedure for  $T^-$  and  $T_2$  preparation is from literature [22]. (a) 5-Mercapto-1-methyltetrazole N-tetramethylammonium salt (TMAT) was prepared by neutralization of 5-mercapto-1-methyltetrazole (1.46 g, 12.6 mmol, 98%; Aldrich) with a 25 wt.%



**Scheme 1.** Synthetic routes and structures of PMIT and  $T_2$ . a) MeOH, TMAOH, Ar, 12 h; b) ACN, PMIBr,  $-18^\circ\text{C}$ ; c)  $H_2O$ ,  $I_2$ , sonicated, 2 h. ACN = acetonitrile, TMAOH = tetramethylammonium hydroxide, PMIBr = 1-methyl-3-propylimidazolium bromide.

solution of tetramethylammonium hydroxide in methanol (1.4 mL, 13.3 mmol; Aldrich) added dropwise in a glove box under an argon atmosphere. The solvent was evaporated, and the resulting white solid was dried under vacuum at 50 °C for 48 h with  $P_2O_5$  (EMD, ACS). (b) TMAI (1.89 g, 10 mmol) was dissolved in acetonitrile, and the white solid TMAI was precipitated by adding 1-methyl-3-propylimidazolium iodide (PMII, 2.27 g, 9 mmol). The solution was kept in the refrigerator for 4 h at –18 °C to reduce the solubility of TMAI. After filtering, the solvent was removed by rotary evaporation. The residue was purified via column chromatography on silica gel, using chloroform/acetone (3:1 v/v) as the eluent. Finally, a colorless liquid (8.1 mmol, 1.9 g, 88%) was obtained after removing the solvent. No impurity was detected by  $^1H$  NMR (300 MHz, Varian).  $^1H$  NMR (300 MHz, DMSO- $d_6$ , ppm):  $\delta$ =3.61 (s, 3H, CH<sub>3</sub>), 9.16 (s, 1H, CH), 7.78–7.70 (m, 2H, CH), 4.153–4.106 (t, 2H, CH<sub>2</sub>), 3.858 (s, 3H, CH<sub>3</sub>), 3.72 (s, 3H, CH<sub>3</sub>), 1.856–1.755 (m, 2H, CH<sub>2</sub>), 0.871–0.822 (t, 3H, CH<sub>3</sub>). TOF ESI (+) EIC mode MS exact mass: calcd for  $C_2H_4N_4S$  = 116.01 ( $M^- + H^+$ ), found = 106.02. +PMI cation: mass: calcd for  $C_7N_2H_{11}I_{13}$  = 125.04 ( $M^+$ ); found = 125.01.

#### 2.4. $T_2$ synthesis [22]

Di-5-(1-methyltetrazole) disulfide ( $T_2$ ) was prepared by oxidizing 5-mercapto-1-methyltetrazole (4.0 g, 34.4 mmol) with iodine (4.0 g, 15.8 mmol, 99.8%; Aldrich) in water. The mixture was sonicated for 1 h until  $I_2$  disappeared. The white precipitate was collected via filtration under vacuum, washed thoroughly with cold nanopure water, and dried under vacuum at 40 °C for 48 h.

### 3. Results and discussions

#### 3.1. Solvent-free and solvated ionic liquid electrolytes for N719-based DSSCs

Solvent-free iodine IL with great potential commercial applications was used to prepare DSSCs [34,37] for its high efficiency and non-volatility. The new synthetic PMIT is a colorless IL. Initially, a pure PMIT IL was used to prepare DSSCs. First, we prepared the  $T_2$ :PMIT (4:10 molar ratio) purely IL electrolyte, and adopted N719 as the sensitizer and a Pt/FTO as the CE to prepare the D1 device. The open-circuit voltage ( $V_{oc}$ ), short-circuit current density ( $J_{sc}$ ), fill factor (FF), and PCE were 630 mV, 10.4 mA cm<sup>-2</sup>, 0.33, and 2.16%, respectively (Fig. 1). Although the PCE has been improved in comparison to previous reports [36], it is still not satisfactory, primarily because of the very low FF. Of the many factors influencing FF, the low diffusion of the redox couple in the electrolyte increases the internal resistance of the cell, causing the FF to decrease [38]. The viscosity of the IL is much higher than that of organic solvents. High viscosity affects the mass transfer process of the electrolyte, which is particularly evident in DSSCs of traditional iodine IL. In particular, the diffusion speed of  $I_3^-$  seriously affects the performance of the devices [32,39,40]. The simplest and most practical method of reducing the viscosity of the electrolyte and increasing the diffusion coefficient of the ion is to add a lower-viscosity general organic solvent or IL [20,35,41,42]. Among these methods, 1-ethyl-3-methylimidazolium tricyanomethanide (EMITCM), which is an IL with lower viscosity and higher conductivity, is widely used in traditional electrolytes based on iodine [42]. We adopted the  $T_2$ :EMITCM:PMIT (4:5:10) electrolyte to prepare the D2 device. The FF of D2 increased from 0.33 to 0.46, and  $V_{oc}$ ,  $J_{sc}$ , and PCE increased to 640 mV, 10.30 mA cm<sup>-2</sup>, and 3.03%, respectively (Fig. 1). Tian et al. [36] adopted a redox couple based on thiadiazole thiolate/disulfide thiadiazole to obtain approximately 1% efficiency under standard illumination conditions [36]. The PCE of the prepared devices D1 and D2 is three times that of the devices

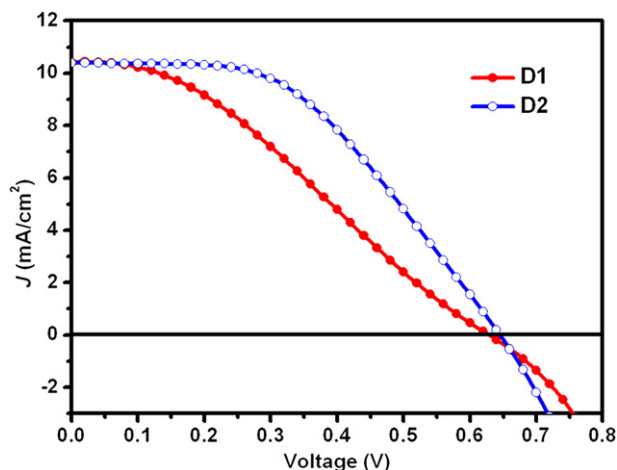
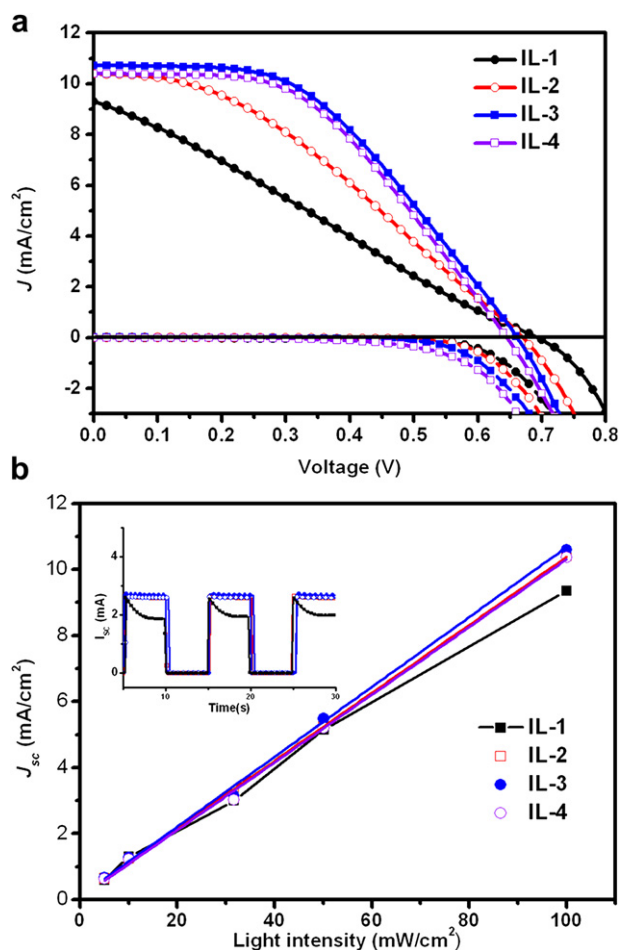


Fig. 1. Photocurrent density–voltage ( $J$ – $V$ ) characteristics of the D1 and D2 devices under AM 1.5 simulated full sunlight (100 mW cm<sup>-2</sup>). Device active area: 0.252 cm<sup>2</sup>. Devices D1 and D2 using  $T_2$ :PMIT (4:10, mol/mol) and  $T_2$ :EMITCM:PMIT (4:5:10, mol/mol) as electrolyte, respectively.

reported by them, which shows the initial advantages of the highly efficient PMIT/ $T_2$  redox couple in iodine-free purely IL DSSCs.

#### 3.2. Recombination and catalytic kinetics of different $T_2$ concentration

After optimization of the ratio of EMITCM:PMIT, a 5.6:10 molar ratio is employed for electrolyte preparation (see Fig. S2). Along with the electrolyte viscosity, the electrolyte composition, especially the proportion of the redox couple, also has a significant effect on the properties of DSSCs [43]. For this reason, we studied the effect of electrolytes with different  $T_2$  contents on cell performance. We found the  $T_2$ :EMITCM:PMIT (2.0:5.6:10) was the optimal ratio (see Table S1). We systematically compared the following binary IL electrolytes: IL1 ( $T_2$ :EMITCM:PMIT = 0.5:5.6:10 molar ratio,  $T_2$ : 0.16 M), IL2 (1.0:5.6:10,  $T_2$ : 0.32 M), IL3 (2:5.6:10,  $T_2$ : 0.64 M), and IL4 (4:5.6:10,  $T_2$ : 1.28 M). Based on these four kinds of IL electrolyte systems, we adopted N719 as the sensitizer and FTO/Pt as the CE to prepare devices IL-1, IL-2, IL-3, and IL-4, respectively. Fig. 2a shows the  $J$ – $V$  curves of IL-1, IL-2, IL-3, and IL-4 under light and dark conditions. Table 1 shows the  $J$ – $V$  performance parameters for the devices. Under standard simulated sunlight,  $J_{sc}$  slightly decreased and remained at the 10 mA cm<sup>-2</sup> level with the increase in  $T_2$  content.  $V_{oc}$  was reduced from 694 to 645 mV, and the FF increased from 0.26 to 0.47. However, the performance of device IL-3 is optimal. Its  $V_{oc}$ ,  $J_{sc}$ , FF, and PCE are 662 mV, 10.7 mA cm<sup>-2</sup>, 0.47, and 3.30%, respectively. To further reveal the effect of different  $T_2$  contents on the recombination dynamics and catalytic kinetics of the devices, we used electrochemical impedance spectroscopy (EIS) to characterize the IL-1, IL-2, IL-3, and IL-4 devices. For the equivalent circuit adopted by the Nyquist plots of corresponding devices, refer to Figs. S3b and S4. The fitting parameter results are shown in Table 1. As shown in Table 1, the charge-transfer resistance ( $R_{CT}$ ) at the counter electrode/electrolyte interface decreased from 38.8  $\Omega$  cm<sup>2</sup> in IL-1 to 11–12  $\Omega$  cm<sup>2</sup> in IL-3 and IL-4 with the increase in  $T_2$  content. The decrease in  $R_{CT}$  is propitious in increasing the FF value, leading to an improvement of the device performance [38]. When the DSSCs were under an open-circuit illumination, the net injection rate of the electron from the excited dyes to TiO<sub>2</sub> was balanced with the recombination of the electron and electrolyte. The open-voltage depends on the electron concentration in the TiO<sub>2</sub> conduction band.  $V_{oc}$  is quantitatively represented by the following equation [44,45]:



**Fig. 2.** (a) Photocurrent density–voltage ( $J$ – $V$ ) characteristics under AM 1.5 simulated full sunlight ( $100 \text{ mW cm}^{-2}$ ) and dark conditions. (b) Light-intensity dependence of the current density of devices IL-1, IL-2, IL-3, and IL-4 under short-circuit condition. The inset shows the short-circuit current–time response ( $100 \text{ mW cm}^{-2}$ ). Sensitizer: N719; counter electrode: FTO/Pt; cell active area:  $0.252 \text{ cm}^2$ .

$$V_{OC} = \frac{kT}{e\mu\alpha} \ln \left( \frac{J_{int}}{\kappa_{rec} n_{c,0}^{\mu\alpha} [T_2]} \right) \quad (1)$$

where  $J_{int}$  refers to the electron injection flow,  $\kappa_{rec}$  refers to the recombination rate constant of  $T_2$ ,  $n_{c,0}$  refers to the electron density of the conduction band of  $\text{TiO}_2$  under dark conditions,  $\mu$  refers to the reaction order of the electrons,  $\alpha$  refers to the electron transfer coefficient,  $[T_2]$  refers to the concentration of the oxidized species,  $k$  refers to Boltzmann constant and  $T$  refers to the absolute

**Table 1**

Detailed photovoltaic parameters of devices IL-1, IL-2, IL-3, and IL-4 under AM 1.5 illumination and EIS parameters. Devices IL-1,2,3 and 4 using IL1,2,3 and 4 as electrolytes, respectively.

Device	$V_{OC}$ (mV)	$J_{sc}$ ( $\text{mA cm}^{-2}$ )	FF	PCE	$R_{CT}^a$ ( $\Omega \text{ cm}^2$ )	$R_{rec}^b$ ( $\Omega \text{ cm}^2$ )	$\tau^c$ (ms)
IL-1	694	9.35	0.26	1.67%	38.8	82.7	60.3
IL-2	670	10.40	0.36	2.49%	20.3	38.9	32.7
IL-3	662	10.71	0.47	3.30%	12.2	26.5	22.8
IL-4	645	10.38	0.47	3.18%	11.4	22.9	18.4

<sup>a</sup>  $R_{rec}$ : recombination resistance at the  $\text{TiO}_2$ -dye/electrolyte interface.

<sup>b</sup>  $R_{CT}$ : charge-transfer recombination resistance at the electrolyte/CE interface. EIS was obtained at the  $-0.65 \text{ V}$  bias voltage under dark conditions.

<sup>c</sup>  $\tau$ : Life time of electrons in photoanode. Device active area:  $0.252 \text{ cm}^2$ ; sensitizer: N719; counter electrode: Pt. IL1 ( $T_2$ :EMITCM:PMIT = 0.5:5.6:10 molar ratio,  $T_2$ : 0.16 M), IL2 (1.0:5.6:10,  $T_2$ : 0.32 M), IL3 (2:5.6:10,  $T_2$ : 0.64 M), and IL4 (4:5.6:10,  $T_2$ : 1.28 M).

temperature. The increase in the content of the oxidized species  $T_2$  enhanced the recombination, which registered as an increase in the dark current density of devices IL-1, IL-2, IL-3, and IL-4 (Fig. 2a) and a decrease in the recombination resistance of the  $\text{TiO}_2$ /electrolyte interface  $R_{rec}$  from  $82.7 \Omega \text{ cm}^2$  in IL-1 to  $22.9 \Omega \text{ cm}^2$  in IL-4. The decrease in the recombination resistance shows that the increased electron recombination rate decreased the life of electron  $\tau$  from 60.3 ms in IL-1 to 18.4 ms in IL-4 (Table 1).  $\tau = R_{rec}C_{\mu}$ , where  $C_{\mu}$  refers to the chemical capacitance that stands for the change of electron density as a function of the Fermi level [46]. These factors caused the electron concentration of  $\text{TiO}_2$  under illumination to decrease, thereby leading to a reduced Fermi energy level,  $E_F$ , of the devices. The  $V_{OC}$  of DSSCs depends on the difference between  $E_F$  and the oxidation–reduction potential  $E_{Red/Ox}$ , thereby reducing the open-circuit voltage. Thus, the  $T_2$  concentration cannot be overly high. However, it also cannot be too low, or it will cause mass transfer problems. Fig. 2b shows the relationship between the short-circuit currents of the four devices and light intensity, as well as the time response curve of short-circuit current under 1.0 sunlight. The short-circuit currents of devices IL-2, IL-3, and IL-4 have a good linear relationship with the light intensity. Hence, no mass transfer problem was observed for the IL-2, IL-3, and IL-4 devices based on the electrolyte. However, device IL-1 deviated from the linearity. The results conform to those of the time response curve of the short-circuit current. The short-circuit current of IL-2, IL-3, and IL-4 almost remained at the maximum level at the beginning of illumination. However, the short-circuit current of IL-1 gradually weakened with time, and was only 75% of the current at the beginning of the illumination at the reaching balance. Therefore, the right  $T_2$  concentration is an important factor in preparing DSSCs with high efficiency and stable output.

The basic requirement for the electrocatalytic performance of the DSSCs cathode is outlined by the typical current densities on  $\text{TiO}_2$  photoanode. Ideally, the exchange-current density on the cathode,  $j_0$ , should be comparable, which provides an estimate of the required charge-transfer resistance,  $R_{CT}$ , of the cathode. The exchange-current density mainly depends on two factors: the concentration of the oxidized species and the electrocatalytic performance of the CE. It is expressed by the exchange-current density,  $j_0$ , of the CE, which is expressed by the following equation [29]:

$$j_0 = \frac{RT}{nFR_{CT}} \quad (2)$$

where  $R$ ,  $T$ ,  $n$  and  $F$  refer to ideal gas constant, absolute temperature, electron-transfer number and Faraday constant. Ideally, the exchange current density provides the required estimated value of the charge-transfer resistance,  $R_{CT}$ . The  $R_{CT}$  of devices IL-1 to IL-4 was clearly reduced with increasing  $T_2$  content, thereby leading to an improved FF. However, this method has limitations. Based on equation (2), when the  $j_0$  of one cell is  $10 \text{ mA cm}^{-2}$ , the  $R_{CT}$  requirement of ideal electrocatalytic materials is around  $2.6 \Omega \text{ cm}^2$ . The results above show that the  $R_{CT}$  value of Pt is far from this requirement. Table 1 shows that the increase of the  $T_2$  content can improve FF by slightly improving the  $R_{CT}$ , albeit at the cost of reducing the  $V_{OC}$ . For efficient DSSCs,  $V_{OC}$  and FF are of equal importance. This needs to increase FF in higher voltage, which is the reason for the need to decrease the internal resistance of cells as much as possible, especially the  $R_{CT}$ . The key to resolving the problem is to find excellent CE materials.

### 3.3. Ink carbon used as CE for D102- and N719-sensitized solar cells

The above-mentioned standard FTO/Pt CE has an excellent catalytic performance for a traditional iodine-based electrolyte.

However, the catalytic performance of the proposed electrolyte containing the sulfur redox couple is not ideal. In previous work, graphite shows better catalytic activity than Pt for  $T_2/T^-$  [47]. Here, we adopted cheaper ink carbon to prepare a carbon CE with 700 nm of thickness in the current study. First, by adopting  $T_2$ :EMITCM:PMIT (1:5.6:10;  $T_2$ : 0.32 M) as the electrolyte, we compared the performance difference between device D-N719-C and device D-N719-Pt using ink carbon and Pt as the CE (Fig. 3a). The  $V_{oc}$ ,  $J_{sc}$ , FF, and PCE of device D-N719-Pt were 670 mV,  $10.4 \text{ mA cm}^{-2}$ , 0.36, and 2.49%, respectively (Table 1). The corresponding parameters of device D-N719-C were 677 mV,  $10.1 \text{ mA cm}^{-2}$ , 0.63, and 4.30%, respectively (Table S2). As far as we know, these are currently the maximum values for IL DSSCs based on an organic redox couple. The  $V_{oc}$  and  $J_{sc}$  of the two devices are very close. After the carbon electrode was adopted, the FF (0.63) of D-N719-C is 1.8 times that of D-N719-Pt (0.36). FF markedly improved, indicating that the ink carbon electrode has a better catalytic performance with this kind of redox couple than Pt. To understand the significant effect of CEs based on FTO/Pt and FTO/ink carbon on the performance of the devices, we studied the EIS of symmetric dummy cells based on a CE//electrolyte//CE structure. The adopted equivalent circuit diagram is shown in Fig. S3a. The  $R_{CT}$  of the ink carbon electrode was  $1.3 \Omega \text{ cm}^2$ , which is 1/24 of the  $R_{CT}$  of the Pt electrode ( $31.6 \Omega \text{ cm}^2$ ). In traditional iodine electrode DSSCs, an important strategy for adopting a carbon electrode to replace Pt is to increase the effective area for charge transfer [i.e., increase the thickness (2–150  $\mu\text{m}$ ) and the specific surface area] [26,29]. However, the thickness of the ink carbon electrode adopted in the current study was around 700 nm and the specific surface was  $30 \text{ m}^2 \text{ g}^{-1}$  (BET). Therefore, the actual catalytic area is much smaller than that of the carbon electrode of traditional iodine-based DSSCs ( $\sim 1000 \text{ m}^2 \text{ g}^{-1}$ ) [48]. The ink carbon material shows excellent electrocatalytic activity for the sulfur-containing redox couple. Recently, Michael Grätzel and co-workers found PEDOT-based counter electrode show good catalytic activity [49]. Thus, abundant and cheap carbon can be used as the electrode for DSSCs in several potential applications. Meanwhile, to compare the difference between the PMIT: $T_2$  electrolyte and traditional iodine IL DSSCs, we prepared the electrolyte  $I_3^-/I^-$  ( $I_2$ :EMITCM:PMII = 1:5.6:10; PMII is 1-methyl-3-propylimidazolium iodide) and prepared the I-N719-C device. Under the same conditions, the  $V_{oc}$ ,  $J_{sc}$ , FF, and PCE of I-N719-C, which has ink carbon as the CE and N719 as the sensitizer, were 658 mV,  $6.36 \text{ mA cm}^{-2}$ , 0.63, and 2.66%, respectively. Its performance is far lower than that of D-N719-C, which is mainly because of the absorption of visible light by the  $I_3^-/I^-$  electrolyte (Fig. S5), thereby causing the decline in  $J_{sc}$ . The new IL redox couple has excellent light transmission, and has potential application in flexible cells based on the rear-illumination mode [50,51]. Meanwhile, D102, a low-cost organic dye, has been successfully applied to DSSCs. The efficiency of liquid-state DSSCs with a Pt CE is 6.1% [52]. We conducted a preliminary study on the new IL redox couple organic dye D102 and the performance of binary IL cells with ink carbon as the CE (Fig. 3a). At standard illumination, the  $V_{oc}$ ,  $J_{sc}$ , FF, and PCE of D-D102-C were 644 mV,  $10.0 \text{ mA cm}^{-2}$ , 0.60, and 3.83%, respectively, which are close to the values of D-N719-C with N719 as the sensitizer. The applicability of the new IL redox couple using an organic dye is evident. In addition, we compared the performance of DSSCs with the new IL redox couple with those of traditional iodine DSSCs under different light intensities. Derived from equation (1), the open-circuit voltage of DSSCs and the light intensity are expressed by the following equation:

$$\frac{dV_{oc}}{d \ln(J_{int})} = \frac{kT}{e\mu\alpha} \quad (3)$$

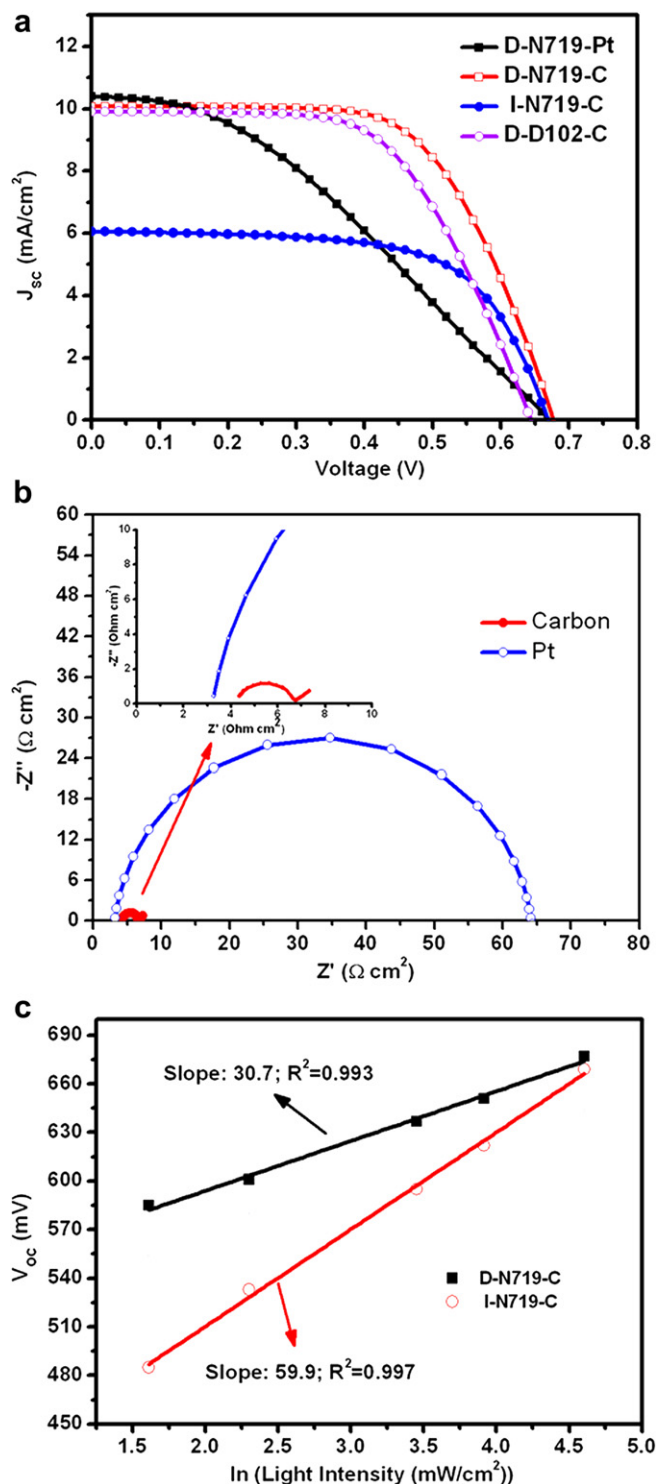


Fig. 3. a) Photocurrent density–voltage ( $J$ – $V$ ) characteristics of D-N719-Pt, D-N719-C, I-N719-C, and D-D102-C under AM 1.5 simulated full sunlight ( $100 \text{ mW cm}^{-2}$ ). (b) Nyquist plots of dummy cells based on FTO/Pt (carbon)//electrolyte//FTO/Pt (carbon) with 0 V bias. (c) Open-circuit voltage ( $V_{oc}$ )–light intensity dependence of D-N719-C and I-N719-C. Device active area:  $0.252 \text{ cm}^2$ .

which reflects the relationship of the recombination dynamics between the electron and the electrolyte. Fig. 3c shows the good linear relationship between  $V_{oc}$  and the natural logarithm of the light intensity of D-N719-C and I-N719-C. Their slopes are 30.7 and 59.9 mV, respectively. Although the difference between the recombination dynamics of these two kinds of electrolytes is still

not clear, this result shows that the electronic recombination rate of the new electrolyte under a weak light intensity is smaller than that of traditional iodine electrolyte DSSCs and that the new electrolyte DSSC has better performance. For example, under  $10 \text{ mW cm}^{-2}$  illumination condition, the efficiencies of D-719-C and D-D102-C under 0.1 sunlight are high (4.90% and 4.30%, respectively), whereas that of I-N719-C was only 2.0%. These results indicate a potential for the devices to operate under dim light (Table S2 and Fig. S6).

#### 4. Conclusions

We synthesized a new IL, 5-mercapto-1-methyltetrazole 1-methyl-3-propylimidazolium (PMIT) to constitute a new, iodine-free, purely IL electrolyte with weak visible light absorption for DSSCs preparation. Adopting Pt as the CE, the energy conversion efficiency was up to 3.30% under standard illumination. By adopting ink carbon as the CE based on the N719 dye, the efficiency reached 4.30% and 4.90% under 1.0 and 0.1 simulated sunlight, respectively. Meanwhile, the low-cost organic dye D102 was also used, and the resulting DSSC efficiency reached 3.83%. These results are currently the maximum efficiency values for IL DSSCs with organic redox couple. We believe that the cell efficiencies will be further boosted with further optimization of the photoanode, especially the adoption of light-scattering layers and further optimization of the dye. Aside from resolving the instability and difficult encapsulation of liquid-state DSSCs, the new organic redox couple IL has the following distinct advantages: first, the EIS results show that the carbon electrode is a more excellent catalyst than Pt for the PMIT/ $\text{I}_2$  redox couple. Therefore, abundant and cheap carbon materials should be widely used to effectively reduce the cost of the cells. Second, the new electrolyte possesses better light transmission and meets the requirement for building integrated photovoltaic. In addition, the new electrolyte is non-corrosive, non-volatile, and environmentally friendly. Third, with better light transmission and easy encapsulation, the new electrolyte has excellent potential application prospects in tandem solar cells [53,54] and flexible solar cells based on rear-illumination [50,51].

#### Acknowledgments

This work was jointly supported by NSFC (50833001), MOST (2011CB933300), and MOE (309001), China.

#### Appendix A. Supplementary data

Supplementary data associated with this article can be found in the online version, at <http://dx.doi.org/10.1016/j.jpowsour.2012.07.067>.

#### References

- [1] B. O'Regan, M. Grätzel, *Nature* 353 (1991) 737–740.
- [2] A. Hagfeldt, M. Grätzel, *Chem. Rev.* 95 (1995) 49–68.
- [3] X. Chen, S.S. Mao, *Chem. Rev.* 107 (2007) 2891–2959.
- [4] A. Mishra, M.K.R. Fischer, P. Bauerle, *Angew. Chem., Int. Ed.* 48 (2009) 2474–2499.
- [5] Y. Ooyama, Y. Harima, *Eur. J. Org. Chem.* (2009) 2903–2934.
- [6] A. Hagfeldt, G. Boschloo, L.C. Sun, L. Kloo, H. Pettersson, *Chem. Rev.* 110 (2010) 6595–6663.
- [7] T.N. Murakami, M. Grätzel, *Inorg. Chim. Acta* 361 (2008) 572–580.
- [8] Q.J. Yu, Y.H. Wang, Z.H. Yi, N.N. Zu, J. Zhang, M. Zhang, P. Wang, *ACS Nano* 4 (2010) 6032–6038.
- [9] M.K. Nazeeruddin, P. Pechy, T. Renouard, S.M. Zakeeruddin, R. Humphry-Baker, P. Comte, P. Liska, L. Cevey, E. Costa, V. Shklover, L. Spiccia, G.B. Deacon, C.A. Bignozzi, M. Grätzel, *J. Am. Chem. Soc.* 123 (2001) 1613–1624.
- [10] F. Gao, Y. Wang, D. Shi, J. Zhang, M.K. Wang, X.Y. Jing, R. Humphry-Baker, P. Wang, S.M. Zakeeruddin, M. Grätzel, *J. Am. Chem. Soc.* 130 (2008) 10720–10728.
- [11] R. Sastrawan, J. Beier, U. Belledin, S. Hemming, A. Hinsch, R. Kern, C. Vetter, F.M. Petrat, A. Prodi-Schwab, P. Lechner, W. Hoffmann, *Sol. Energy Mater. Sol. Cells* 90 (2006) 1680–1691.
- [12] K. Okada, H. Matsui, T. Kawashima, T. Ezure, N. Tanabe, *J. Photochem. Photobiol., A* 164 (2004) 193–198.
- [13] H. Nusbaumer, J.E. Moser, S.M. Zakeeruddin, M.K. Nazeeruddin, M. Grätzel, *J. Phys. Chem. B* 105 (2001) 10461–10464.
- [14] S.A. Sapp, C.M. Elliott, C. Contado, S. Caramori, C.A. Bignozzi, *J. Am. Chem. Soc.* 124 (2002) 11215–11222.
- [15] S. Cazzanti, S. Caramori, R. Argazzi, C.M. Elliott, C.A. Bignozzi, *J. Am. Chem. Soc.* 128 (2006) 9996–9997.
- [16] E.A. Gibson, A.L. Smeigh, L. Le Pleux, J. Fortage, G. Boschloo, E. Blart, Y. Pellegrin, F. Odobel, A. Hagfeldt, L. Hammarstrom, *Angew. Chem., Int. Ed.* 48 (2009) 4402–4405.
- [17] T. Daeneke, T.H. Kwon, A.B. Holmes, N.W. Duffy, U. Bach, L. Spiccia, *Nat. Chem.* 3 (2011) 211–215.
- [18] C. Teng, X.C. Yang, C.Z. Yuan, C.Y. Li, R.K. Chen, H.N. Tian, S.F. Li, A. Hagfeldt, L.C. Sun, *Org. Lett.* 11 (2009) 5542–5545.
- [19] G. Oskam, B.V. Bergeron, G.J. Meyer, P.C. Searson, *J. Phys. Chem. B* 105 (2001) 6867–6873.
- [20] P. Wang, S.M. Zakeeruddin, J.E. Moser, R. Humphry-Baker, M. Grätzel, *J. Am. Chem. Soc.* 126 (2004) 7164–7165.
- [21] Z. Zhang, P. Chen, T.N. Murakami, S.M. Zakeeruddin, M. Grätzel, *Adv. Funct. Mater.* 18 (2008) 341–346.
- [22] M.K. Wang, N. Chamberland, L. Breau, J.E. Moser, R. Humphry-Baker, B. Marsan, S.M. Zakeeruddin, M. Grätzel, *Nat. Chem.* 2 (2010) 385–389.
- [23] H.N. Tian, X.A. Jiang, Z. Yu, L. Kloo, A. Hagfeldt, L.C. Sun, *Angew. Chem., Int. Ed.* 49 (2010) 7328–7331.
- [24] Y. Liu, J.R. Jennings, M. Parameswaran, Q. Wang, *Energy Environ. Sci.* 4 (2011) 564–571.
- [25] D.F. Zhou, Q.J. Yu, N. Cai, Y. Bai, Y.H. Wang, P. Wang, *Energy Environ. Sci.* 4 (2011) 2030–2034.
- [26] T.N. Murakami, S. Ito, Q. Wang, M.K. Nazeeruddin, T. Bessho, I. Cesar, P. Liska, R. Humphry-Baker, P. Comte, P. Pechy, M. Grätzel, *J. Electrochem. Soc.* 153 (2006) A2255–A2261.
- [27] K. Imoto, M. Suzuki, K. Takahashi, T. Yamaguchi, T. Komura, J. Nakamura, K. Murata, *Electrochemistry* 71 (2003) 944–946.
- [28] G.Q. Wang, W. Xing, S.P. Zhuo, *J. Power Sources* 194 (2009) 568–573.
- [29] L. Kavan, J.H. Yum, M. Grätzel, *ACS Nano* 5 (2011) 165–172.
- [30] Q.W. Jiang, G.R. Li, X.P. Gao, *Chem. Commun.* (2009) 6720–6722.
- [31] M.K. Wang, A.M. Anghel, B. Marsan, N.L.C. Ha, N. Pootrakulchote, S.M. Zakeeruddin, M. Grätzel, *J. Am. Chem. Soc.* 131 (2009) 15976–15977.
- [32] N. Papageorgiou, Y. Athanassov, M. Armand, P. Bonhôte, H. Pettersson, A. Azam, M. Grätzel, *J. Electrochem. Soc.* 143 (1996) 3099–3108.
- [33] P. Wang, S.M. Zakeeruddin, P. Comte, I. Exnar, M. Grätzel, *J. Am. Chem. Soc.* 125 (2003) 1166–1167.
- [34] D.B. Kuang, P. Wang, S. Ito, S.M. Zakeeruddin, M. Grätzel, *J. Am. Chem. Soc.* 128 (2006) 7732–7733.
- [35] Y. Bai, Y.M. Cao, J. Zhang, M. Wang, R.Z. Li, P. Wang, S.M. Zakeeruddin, M. Grätzel, *Nat. Mater.* 7 (2008) 626–630.
- [36] L. Kloo, H.N. Tian, Z. Yu, A. Hagfeldt, L. Sun, *J. Am. Chem. Soc.* 133 (2011) 9413–9422.
- [37] S.M. Zakeeruddin, M. Grätzel, *Adv. Funct. Mater.* 19 (2009) 2187–2202.
- [38] M. Murayama, T. Mori, *Jpn. J. Appl. Phys. Part 1* 45 (2006) 542–545.
- [39] W. Kubo, S. Kambe, S. Nakade, T. Kitamura, K. Hanabusa, Y. Wada, S. Yanagida, *J. Phys. Chem. B* 107 (2003) 4374–4381.
- [40] W. Kubo, T. Kitamura, K. Hanabusa, Y. Wada, S. Yanagida, *Chem. Commun.* (2002) 374–375.
- [41] P. Wang, S.M. Zakeeruddin, R. Humphry-Baker, M. Grätzel, *Chem. Mater.* 16 (2004) 2694–2696.
- [42] P. Wang, B. Wenger, R. Humphry-Baker, J.E. Moser, J. Teuscher, W. Kanteleiner, J. Mezger, E.V. Stoyanov, S.M. Zakeeruddin, M. Grätzel, *J. Am. Chem. Soc.* 127 (2005) 6850–6856.
- [43] G. Boschloo, A. Hagfeldt, *Acc. Chem. Res.* 42 (2009) 1819–1826.
- [44] S.Y. Huang, G. Schlichthorl, A.J. Nozik, M. Grätzel, A.J. Frank, *J. Phys. Chem. B* 101 (1997) 2576–2582.
- [45] A. Kumar, P.G. Santangelo, N.S. Lewis, *J. Phys. Chem.* 96 (1992) 834–842.
- [46] G. Schlichthorl, S.Y. Huang, J. Sprague, A.J. Frank, *J. Phys. Chem. B* 101 (1997) 8141–8155.
- [47] H. Wu, Z. Lv, Z. Chu, D. Wang, S. Hou, D. Zou, *J. Mater. Chem.* (2011).
- [48] S.Q. Fan, B. Fang, J.H. Kim, B. Jeong, C. Kim, J.S. Yu, J. Ko, *Langmuir* 26 (2010) 13644–13649.
- [49] J. Burschka, V. Brault, S. Ahmad, L. Breau, M.K. Nazeeruddin, B. Marsan, S.M. Zakeeruddin, M. Grätzel, *Energy Environ. Sci.* 5 (2012) 6089–6097.
- [50] X. Fan, Z.Z. Chu, F.Z. Wang, C. Zhang, L. Chen, Y.W. Tang, D.C. Zou, *Adv. Mater.* 20 (2008) 592.
- [51] Z.B. Lv, Y.P. Fu, S.C. Hou, D. Wang, H.W. Wu, C. Zhang, Z.Z. Chu, D.C. Zou, *Phys. Chem. Chem. Phys.* 13 (2011) 10076–10083.
- [52] T. Horiuchi, H. Miura, S. Uchida, *Chem. Commun.* (2003) 3036–3037.
- [53] J.J. He, H. Lindstrom, A. Hagfeldt, S.E. Lindquist, *Sol. Energy Mater. Sol. Cells* 62 (2000) 265–273.
- [54] A. Nattestad, A.J. Mozer, M.K.R. Fischer, Y.B. Cheng, A. Mishra, P. Bauerle, U. Bach, *Nat. Mater.* 9 (2010) 31–35.